Propofol inhibits the malignant development of osteosarcoma U2OS cells via AMPK/FOXO1-mediated autophagy

LINA DAI[1], SHIMEI LI[1], XI LI[1] and BO JIANG[2]

[1]Department of Anesthesiology, The First Affiliated Hospital of Guizhou University of Traditional Chinese Medicine, Guiyang, Guizhou 550001; [2]Department of Orthopedic and Sports Medicine, Ningbo First Hospital, Ningbo, Zhejiang 315000, P.R. China

Abstract. It has previously been reported that propofol regulates the development of human osteosarcoma (OS). However, the specific molecular mechanisms underlying the effect of propofol on OS remain poorly understood. Therefore, the aim of the present study was to explore the effects of propofol on OS U2OS cells and the potential underlying mechanism. The Cell Counting Kit-8 and colony formation assays were performed to assess cell viability and proliferation. Furthermore, cell apoptosis was assessed using the TUNEL assay and western blotting. Wound healing and Transwell assays were performed to evaluate OS cell migration and invasion abilities, respectively. The protein expression levels of epithelial-mesenchymal transition (EMT)-, autophagy- and adenosine monophosphate-activated protein kinase (AMPK)/FOXO1 signaling pathway-related proteins were also determined using western blotting. The results demonstrated that propofol significantly reduced the viability of OS cells and promoted autophagy in a dose-dependent manner. Moreover, cell treatment with propofol significantly enhanced the protein expression levels of phosphorylated (p)-AMPK and FOXO1, while decreasing the protein levels of p-FOXO1. Furthermore, treatment with propofol significantly suppressed cell viability, migration and invasion abilities and the EMT of OS cells, and potentially promoted cell apoptosis via inducing autophagy via the AMPK/FOXO1 signaling pathway. In summary, the present study indicated that propofol potentially had an inhibitory effect on the development of OS cells via AMPK/FOXO1-mediated autophagy. These results have therefore provided an experimental basis for further studies into the therapeutic effect of propofol on OS.

Correspondence to: Dr Bo Jiang, Department of Orthopedic and Sports Medicine, Ningbo First Hospital, 59 Liuting Street, Ningbo, Zhejiang 315000, P.R. China
E-mail: jiangbojj@126.com

Introduction

Osteosarcoma (OS), a malignant tumor originating from the mesenchymal tissue, commonly occurs in children and adolescents (1-3). OS may only be accompanied by local pain and swelling. However, pulmonary metastasis from OS is likely to occur at an early stage of the disease and develops rapidly (4). With surgical procedures and the application of chemotherapy, the 5-year survival rate has improved significantly (5). However, further improvement of therapeutics of OS has been limited, especially for patients with lung metastasis (6). Therefore, identifying novel therapeutic methods and strategies for the treatment of OS and its development is of importance.

Anesthetic agents may serve an essential role in tumor relapse and metastasis as they are administered at the moment of greatest risk of transmission, which is the surgical removal of the tumor (7). Recently, numerous studies have reported that the type of anesthetic agent used could influence the prognosis of patients with cancer undergoing surgery for cancer treatment (8,9). Propofol, a common intravenous anesthetic, is commonly used for anesthesia prior to tumor resection (10). Emerging evidence suggests that propofol can inhibit the growth and metastasis of tumor cells (11,12). Propofol can enhance the anti-tumor effect of chemotherapeutic drugs or certain small molecular compounds (13). Furthermore, *in vivo* animal models have demonstrated that propofol suppresses tumor growth and metastasis (14). It has also been demonstrated in clinical trials that propofol is associated with better survival rates in patients with cancer following surgery (15,16). Therefore, it is important to study the effects of propofol on numerous types of cancer and its potential underlying mechanisms.

Previous studies have reported that propofol is involved in tumor development via modulation of the expression of key RNAs, such as microRNAs (miRs) and long non-coding RNAs (lncRNAs), and the activation of several signaling pathways, including the hypoxia-inducible factor-1α, MAPK, NF-κB and nuclear factor E2-related factor-2 signaling pathways (17-19). Moreover, it has been demonstrated that propofol affects the degree of host immunosuppression and modulates immune function (20). It has also been reported that propofol has a regulatory effect on the proliferation, invasion and apoptosis

of OS cells (21,22). However, the specific molecular mechanisms underlying the effect of propofol on OS remain unclear.

Autophagy is an evolutionarily conserved catabolic process that maintains cellular homeostasis via degrading long-lived and damaged proteins or organelles in cells (23). Emerging evidence has suggested that autophagy can inhibit the malignant development of OS (24). Furthermore, a previous study has reported that propofol can benefit organs and tissues in cancer by modulating autophagy, which is an evolutionarily conserved catabolic process that maintains cellular homeostasis by degrading long-lived proteins and damaged cellular proteins or organelles (25).

Therefore, the aim of the present study was to investigate whether propofol inhibited the development of OS via inducing cell autophagy. Furthermore, whether the adenosine monophosphate-activated protein kinase (AMPK)/FOXO1 signaling pathway was involved in the regulation of autophagy in OS was also explored.

Materials and methods

Cell culture and treatment. The human OS U2OS cell line was purchased from the American Type Culture Collection. Cells were cultured in DMEM (Gibco; Thermo Fisher Scientific, Inc.) supplemented with 10% FBS (Gibco; Thermo Fisher Scientific, Inc.), 100 μg/ml streptomycin and 100 U/ml penicillin at 37°C in a humidified atmosphere with 5% CO_2. U2OS cells were treated with different concentrations (0, 2.5, 5 and 10 μg/ml) of propofol (MilliporeSigma) at 37°C for 48 h (26-28). Untreated cells were used as the control. To reveal the underlying molecular mechanism of propofol, U2OS cells were also co-treated with 10 μg/ml propofol with or without 20 μM compound C (MedChemExpress), an antagonist of AMPK, with or without 50 nM rapamycin (RAP; Abcam), an autophagy agonist, for 24 h at 37°C.

Cell counting kit 8 (CCK-8) assay. U2OS cells under different treatment conditions were cultured in DMEM with 10% FBS at 37°C for 24 h. Subsequently, 10 μl CCK-8 solution (Dojindo Laboratories, Inc.) was added into each well and the cells ($5x10^3$ cells/well) were incubated for 2 h. The absorbance of each well was assessed at a wavelength of 450 nm using a microplate reader (Bio-Rad Laboratories, Inc.). A total of six parallel wells were used for each group.

Colony formation assay. U2OS cells under different treatment conditions were seeded into 6-well plates (500 cells/well) and incubated in DMEM with 10% bovine calf serum (Thermo Fisher Scientific, Inc.) at 37°C. The medium was replaced with fresh complete culture medium every 3 days, and the cells were incubated for 2 weeks. The cells were fixed with 4% paraformaldehyde for 20 min at room temperature and stained with 0.1% crystal violet solution for 30 min at room temperature. A cell group containing >50 cells was identified as a colony. The number of visible colonies was counted manually using a light microscope (Olympus Corporation). All experiments were repeated three times.

TUNEL assay. Cell apoptosis was assessed using the TUNEL assay. An *in situ* Cell Death Detection Kit (Roche Diagnostics GmbH) was used according to the manufacturer's instructions. Briefly, U2OS cells ($2x10^5$ cells/well) in a 24-well plate under different treatment conditions were fixed with 4% paraformaldehyde at room temperature for 30 min and incubated with proteinase K for 15 min at 37°C. Subsequently, the cells were incubated with 3% H_2O_2 for 15 min at room temperature and were then treated using the *in situ* Cell Death Detection Kit for 60 min at 37°C. Following incubation, cells were co-labeled with 1 μg/ml DAPI working solution for 10 min in the dark. Slides were mounted using glycerol. Apoptotic cells in six randomly selected fields of view were imaged using a fluorescence microscope (Leica Microsystems GmbH) and quantified by ImageJ Software (version 6.0; National Institutes of Health).

Wound healing assay. U2OS cell migration ability was assessed using a wound healing assay. Briefly, U2OS cells under different treatment conditions were seeded into a 6-well plate ($1x10^5$ cells/well) and cultured in serum-free DMEM until they reached 90% confluency. Subsequently, a straight scratch was made on the cell monolayer using a 20-μl pipette tip followed by washing with serum-free medium three times. Following incubation for 24 h, the cell migration rate was calculated using the following formula: (wound width at 0 h-wound width at 24 h)/wound width at 0 h x 100. Images were captured by a light Nikon ECLIPSE E100 microscope and the gap distance was quantitatively evaluated using ImageJ software (version 1.8.0 172; National Institutes of Health).

Transwell assay. Cell invasion ability was assessed using the Transwell assay. The Transwell chambers (Costar; Corning, Inc.) were first coated with 0.1 ml Matrigel (BD Biosciences) at 37°C for 1 h. U2OS cells under different treatment conditions were suspended in serum-free DMEM at a final concentration of $5x10^5$ cells/ml and seeded into the upper chamber, whereas the lower chamber was supplemented with DMEM containing 5% FBS. Following incubation for 24 h at 37°C, cells on the lower surface of the membrane were fixed with 100% methanol at room temperature for 20 min and stained with 0.1% crystal violet for 15 min at room temperature. Invaded cells were counted using an inverted light microscope and analyzed using ImageJ software (version 1.8.0 172; National Institutes of Health).

Western blotting. Total protein was extracted from U2OS cells under different treatment conditions using RIPA buffer (Auragene; Hunan Aijia Biotechnology Co., Ltd.) and protein concentration was quantified using the BCA method (Thermo Fisher Scientific, Inc.). Total protein (50 μg/lane) was separated using SDS-PAGE on a 10% gel and separated proteins were then electrotransferred onto PVDF membranes. Following blocking with 5% non-fat milk for 1 h at room temperature, the membranes were incubated at 4°C overnight with the following primary antibodies against: LC3II/I (cat. no. 14600-1-AP; 1:1,000; ProteinTech Group, Inc.), Beclin1 (cat. no. ab207612; 1:2,000; Abcam), p62 (cat. no. ab207305; 1:1,000; Abcam), phosphorylated (p)-AMPK (cat. no. ab133448; 1:1,000; Abcam), AMPK (cat. no. ab32047; 1:1,000; Abcam), p-FOXO1 (cat. no. ab131339; 1:1,000; Abcam), FOXO1
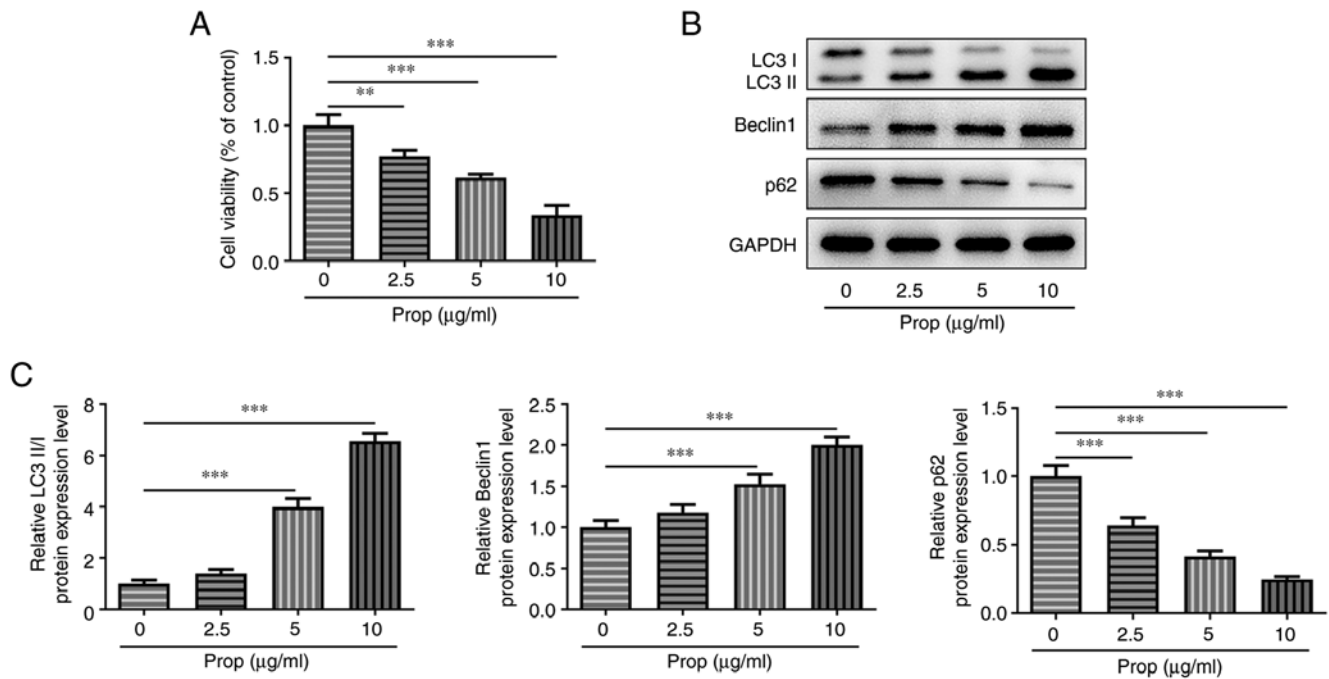
Figure 1. Prop inhibits cell viability and induces cell autophagy in U2OS cells. (A) Cell viability was detected using the Cell Counting Kit-8 assay. (B) Protein expression levels of LC3II/I, Beclin1 and p62 were determined using western blotting. (C) Semi-quantification of the related western blotting bands. Data are presented as the mean ± SD. **P<0.01 and ***P<0.001. Prop, propofol.
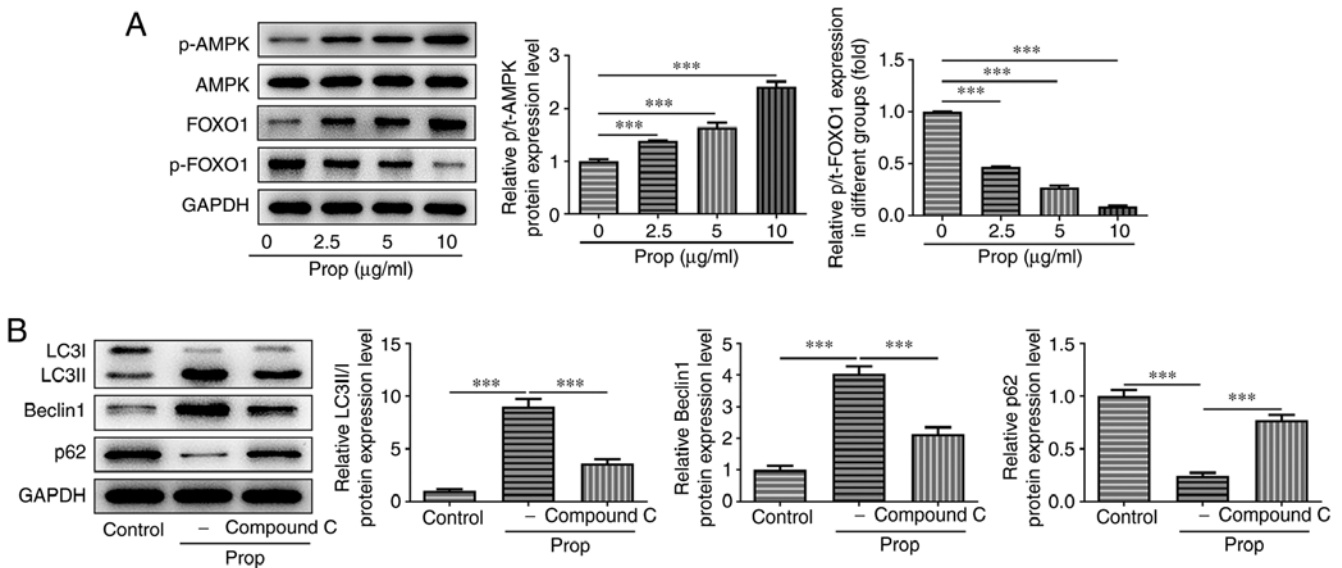

Figure 2. Prop induces the autophagy of U2OS cells by activating the AMPK/FOXO1 signaling pathway. (A) Protein expression levels of t-AMPK, p-AMPK, FOXO1 and p-FOXO1 were detected via western blotting. (B) Protein expression levels of LC3II/I, Beclin1 and p62 were detected via western blotting. Data are presented as the mean ± SD. ***P<0.001. Prop, propofol; AMPK, adenosine monophosphate-activated protein kinase; t, total; p, phosphorylated.

(cat. no. ab179450; 1:1,000; Abcam), Bcl-2 (cat. no. ab32124; 1;1,000; Abcam), Bax (cat. no. ab32503; 1:1,000; Abcam), cleaved caspase-3 (cat. no. ab32042; 1:500; Abcam), caspase-3 (cat. no. ab32351; 1:5,000; Abcam), N-cadherin (cat. no. ab76011; 1:5,000; Abcam), Vimentin (cat. no. ab92547; 1:1,000; Abcam), E-cadherin (cat. no. ab40772; 1:10,000; Abcam) and GAPDH (cat. no. ab9485; 1:2,500; Abcam). Following washing three times with TBS-0.1% Tween 20, the membranes were incubated with the corresponding horseradish peroxidase-conjugated secondary antibodies

(cat. no. 7074; 1:1,000; Cell Signaling Technology, Inc.) for 1 h at room temperature. Separated proteins were visualized using an enhanced chemiluminescence detection system (Amersham; Cytiva). ImageJ software (version 1.8.0 172; National Institutes of Health) was used to analyze the images. The data were normalized to GAPDH to obtain the integral optical density values.

Statistical analysis. All experiments were repeated three times. All statistical analysis was performed using SPSS
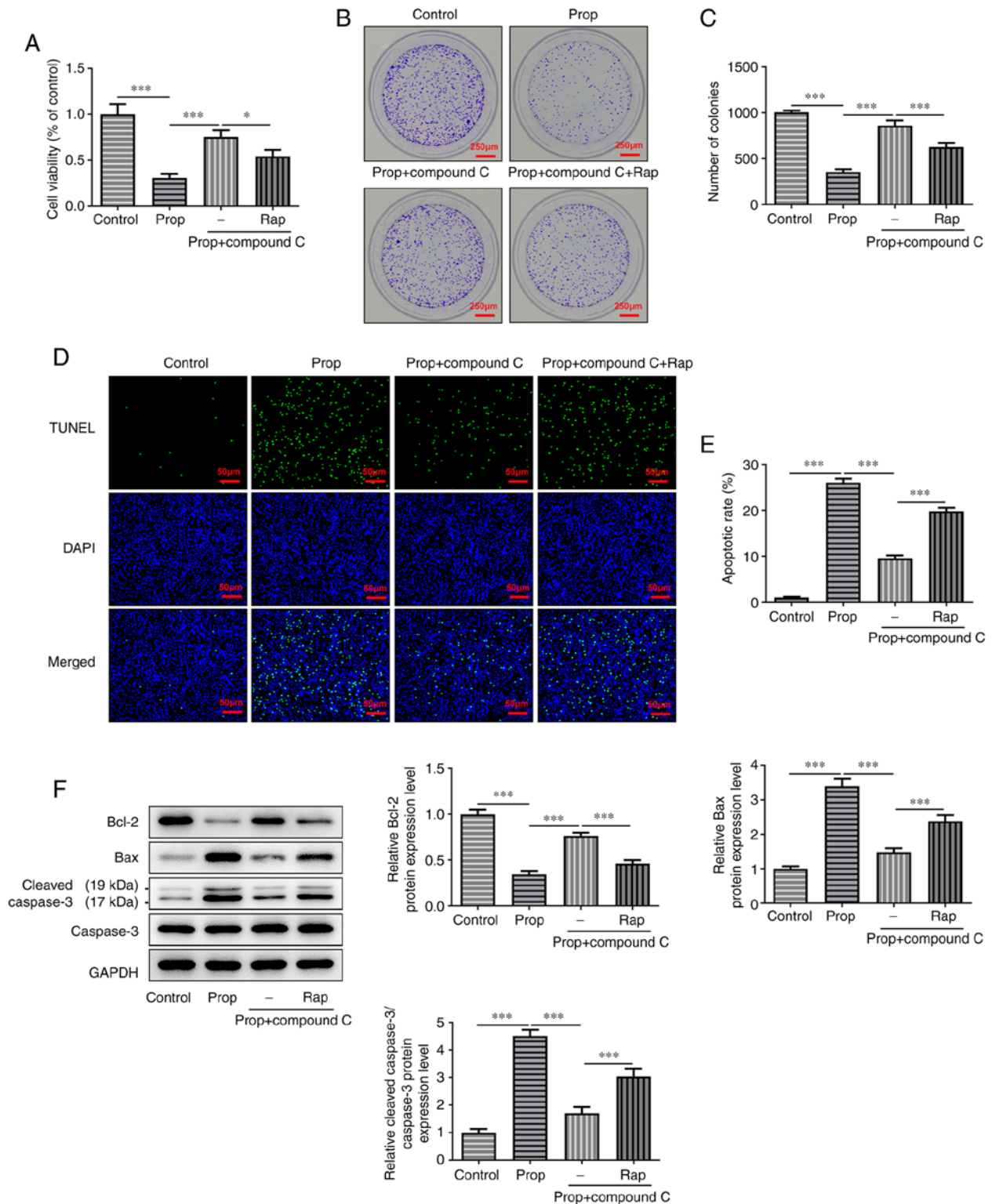
Figure 3. Prop induces adenosine monophosphate-activated protein kinase/FOXO1 pathway-mediated autophagy to inhibit cell proliferation and promote apoptosis in U2OS cells. (A) Cell viability was detected using the Cell Counting Kit-8 assay. (B) Cell proliferation was assessed using the colony formation assay. (C) Quantification of cell colony number. (D) Cell apoptosis was assessed using the TUNEL assay. Scale bar, 50 μm. (E) Quantification of the U2OS cell apoptotic rate. (F) Protein expression levels of Bcl-2, Bax, caspase-3 and cleaved caspase-3 were detected via western blotting. Data are presented as the mean ± SD. *P<0.05 and ***P<0.001. Prop, propofol; RAP, rapamycin.

22.0 software (IBM Corp.). All data are presented as the mean ± SD. The differences among multiple groups were analyzed using one-way ANOVA followed by Bonferroni's multiple comparison post hoc test. P<0.05 was considered to indicate a statistically significant difference.

Results

Propofol attenuates U2OS cell viability and promotes cell autophagy. To explore the effects of propofol on OS cells, the present study first investigated the effect of different doses
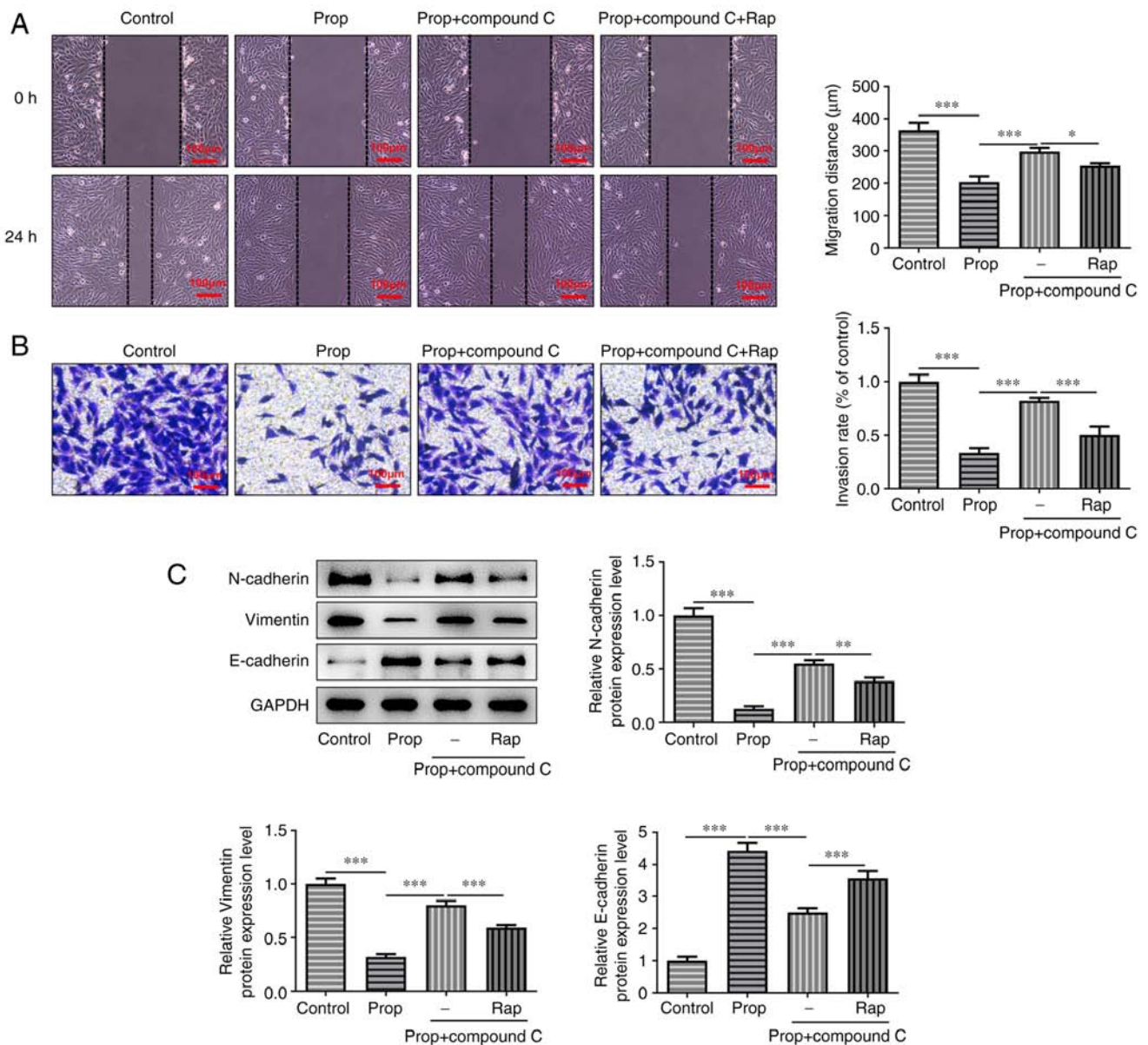
Figure 4. Prop inhibits U2OS cell migration, invasion and the epithelial-mesenchymal transition via autophagy through the activation of the adenosine monophosphate-activated protein kinase/FOXO1 signaling pathway. (A) Cell migration was analyzed using the wound healing assay. (B) Cell invasion was assessed using the Transwell assay. (C) N-cadherin, Vimentin and E-cadherin protein expression levels were detected via western blotting. Data are presented as the mean ± SD. *P<0.05, **P<0.01 and ***P<0.001. Prop, propofol.

of propofol on U2OS cell viability. The results demonstrated that compared with untreated cells, U2OS cell viability was significantly reduced in a dose-dependent manner following cell treatment with different doses of propofol (Fig. 1A). Furthermore, treatment with propofol significantly upregulated LC3II/I and Beclin1 protein expression levels at 5 and 10 µg/ml and significantly downregulated p62 protein expression levels at all doses, compared with the untreated control. These results therefore indicated that propofol may promote U2OS cell autophagy (Fig. 1B and C).

Propofol promotes U2OS cell autophagy via dose-dependent activation of the AMPK/FOXO1 signaling pathway. Subsequently, the present study aimed to investigate how propofol affected U2OS cell autophagy. Western blotting demonstrated that treatment with propofol significantly

increased the protein expression levels of p-AMPK in a dose-dependent manner compared with the untreated control, whereas the total levels of AMPK remained unchanged. Furthermore, compared with the untreated control, the protein expression levels of total FOXO1 were significantly increased in a dose-dependent manner, whereas those of p-FOXO1 were significantly reduced following cell treatment with increasing concentrations of propofol (Fig. 2A). Cells were also treated with 20 µM compound C, an AMPK/FOXO1 signaling pathway inhibitor. The results demonstrated that the protein expression levels of LC3II/I and Beclin1 were significantly reduced, whereas those of p62 were significantly elevated in cells co-treated with propofol and compound C, compared with cells treated only with propofol (Fig. 2B). These results suggested that the AMPK/FOXO1 signaling pathway may be involved in propofol-induced autophagy in U2OS cells.

Propofol attenuates cell proliferation and promotes apoptosis via AMPK/FOXO1 signaling pathway-induced autophagy in U2OS cells. To explore the effects of propofol-induced autophagy on cell proliferation and apoptosis, U2OS cells were treated with 50 nM RAP. The results of the CCK-8 assay demonstrated that co-treatment of U2OS cells with propofol and compound C significantly promoted cell viability compared with cells treated with propofol only. However, RAP significantly reversed the effects of compound C on cell viability compared with the propofol + compound C group (Fig. 3A). Furthermore, the colony formation assay demonstrated that co-treatment of propofol and compound C significantly increased the number of cell colonies compared with the propofol group. However, the additional treatment with RAP significantly reversed this increase in U2OS cell colonies compared with the propofol + compound C group (Fig. 3B and C). The results of the TUNEL assay demonstrated that cell apoptosis was significantly increased in propofol-treated cells compared with the control group. However, cell co-treatment with compound C significantly attenuated propofol-induced cell apoptosis compared with the propofol only group, whereas RAP significantly reversed the inhibitory effect of compound C on U2OS cell apoptosis compared with the propofol + compound C group (Fig. 3D and E). Furthermore, cell treatment with compound C significantly promoted Bcl-2 protein expression levels and significantly downregulated the protein expression levels of Bax and cleaved caspase-3 compared with the propofol only group. However, the protein expression levels of the aforementioned proteins were significantly reversed following cell treatment with RAP compared with the propofol + compound C group (Fig. 3F). In summary, propofol hindered the occurrence of OS via modulation of AMPK/FOXO1 signaling pathway-induced autophagy.

Propofol suppresses U2OS cell migration, invasion and the epithelial-mesenchymal transition (EMT) via autophagy through the activation of the AMPK/FOXO1 signaling pathway. Subsequently, the effects of propofol-induced autophagy on cell migration, invasion and the EMT were assessed. The results demonstrated that propofol significantly inhibited cell migration and invasion compared with the untreated control group, which was significantly reversed by cell treatment with compound C (Fig. 4A and B). The effect of compound C on enhancing cell invasion was markedly abrogated and on enhancing cell migration was slightly reduced following cell treatment with RAP, compared with the propofol + compound C group. Furthermore, western blotting demonstrated that the protein expression levels of N-cadherin and Vimentin were significantly reduced, whereas those of E-cadherin were significantly enhanced by propofol treatment compared with the control group. However, inhibition of the AMPK/FOXO1 signaling pathway using compound C significantly reversed these results compared with the propofol only group. Furthermore, cell treatment with RAP resulted in a significant inverse effect on the protein expression levels of N-cadherin, Vimentin and E-cadherin compared with the propofol + compound C group. In conclusion, propofol impeded the progression of OS via modulation of AMPK/FOXO1 signaling pathway-induced autophagy.

Discussion

OS is an aggressive type of malignant tumor that often occurs in young individuals (29). OS is characterized by a high metastatic rate and drug resistance, which therefore leads to a high mortality rate (30). The present study investigated the effect of propofol on human OS cells and its potential underlying molecular mechanism. The results demonstrated that propofol significantly inhibited cell viability, migration, invasion and the EMT, and significantly promoted U2OS cell apoptosis. Furthermore, the results demonstrated that AMPK/FOXO1-mediated autophagy may be involved in the mechanism of propofol on OS, which therefore suggested that propofol may potentially serve a crucial role in OS progression via AMPK/FOXO1-mediated autophagy.

Propofol is an intravenous anesthetic that is commonly used in clinical practice and it has been reported to inhibit the development of several types of cancer, including breast cancer, gastric cancer and colon cancer (12,31,32). Ye *et al* (28) demonstrated that propofol attenuates the proliferation and invasion and promotes the apoptosis of OS cells via the upregulation of miR-143. Furthermore, Xu *et al* (21) reported that propofol could downregulate TGF-β1 expression, which results in the inhibition of the proliferation and invasion of OS cells. In the present study, propofol significantly reduced U2OS cell viability in a dose-dependent manner. Moreover, TUNEL assays and western blotting demonstrated that propofol significantly promoted cell apoptosis and modulated the protein expression levels of Bcl-2, Bax and cleaved caspase-3, respectively. Wound healing and Transwell assays demonstrated that propofol significantly reduced the migration and invasion abilities and suppressed the EMT process in U2OS cells, which was consistent with previous studies (21,28).

Autophagy can function as an important process that can inhibit the malignant development of OS (33). A previous study reported that propofol serves a beneficial role in organs and tissues via the regulation of autophagy (34). Propofol also regulates cancer cell autophagy (35). For example, Zhang *et al* (36) demonstrated that propofol could improve gastric cancer cell sensitivity to cisplatin via lncRNA metastasis-associated lung adenocarcinoma transcript 1/miR-30e/autophagy related 5 axis-mediated autophagy. Furthermore, Wang *et al* (35) reported that propofol inhibits cell proliferation and the cell cycle but promotes cell apoptosis during hepatocarcinogenesis via the activation of AMPK and the induction of autophagy, both *in vivo* and *in vitro*. In the present study, the protein expression levels of autophagy-related proteins were detected via western blotting. The results demonstrated that propofol may have promoted autophagy via the significant upregulation of LC3II/I and Beclin1 and the downregulation of p62 protein expression levels. However, transmission electron microscopy and GFP-LC3 fluorescence assays may better locate autophagy-related proteins and therefore these methods will be used to investigate the effect of propofol on cell autophagy in future work.

Emerging evidence has suggested that inhibiting the FOXO1/tumor suppressor candidate 7 axis via regulating the AKT/GSK-3β signal transduction pathway can decrease the proliferation, migration and invasion abilities of OS

cells (22). Huang *et al* (22) reported that propofol could increase the transcriptional activity of FOXO1. FOXO1 serves a key role in autophagy in cancer cells (37,38). A previous study demonstrated that trichostatin A induced cell autophagy via activating the transcriptional activity of FOXO1 in OS (39). Furthermore, Chen *et al* (40) demonstrated that propofol could attenuate HeLa cell growth via impairing autophagic flux via AMPK activation and calcium-regulated endoplasmic reticulum stress. The present study demonstrated that autophagy may be promoted in OS cell treatment with propofol via the activation of the AMPK/FOXO1 signaling pathway. Furthermore, propofol potentially enhanced AMPK/FOXO1 pathway-mediated autophagy to inhibit OS cell proliferation and metastasis and promote cell apoptosis. It should be noted that animal and clinical trials are more complex and uncontrollable than cell experiments. Therefore the dose of propofol used in clinical trials does not apply to the doses used in the present study. Furthermore, there may be other signaling pathways that are regulated by propofol in OS, which will be investigated in future work.

To the best of our knowledge the present study was the first to provide evidence that propofol potentially regulated OS progression via AMPK/FOXO1 pathway-mediated autophagy. This has therefore provided a novel insight into the potential effect of propofol in the treatment of OS.

Acknowledgements

Not applicable.

Funding

Availability of data and materials

The datasets used and/or analyzed during the current study are available from the corresponding author on reasonable request.

Authors' contributions

LD and BJ designed the study, drafted and revised the manuscript. LD, SL and XL performed the experiments, searched the literature and analyzed the data. BJ guided the experiments. All authors read and approved the final manuscript. LD and BJ confirm the authenticity of all the raw data.

Ethics approval and consent to participate

Not applicable.

Patients consent for publication

Not applicable.

Competing interests

The authors declare that they have no competing interests.

References

1. Harrison DJ, Geller DS, Gill JD, Lewis VO and Gorlick R: Current and future therapeutic approaches for osteosarcoma. Expert Rev Anticancer Ther 18: 39-50, 2018.
2. Eaton BR, Schwarz R, Vatner R, Yeh B, Claude L, Indelicato DJ and Laack N: Osteosarcoma. Pediatr Blood Cancer 68 (Suppl 2): e28352, 2021.
3. Corre I, Verrecchia F, Crenn V, Redini F and Trichet V: The Osteosarcoma microenvironment: A complex but targetable ecosystem. Cells 9: 976, 2020.
4. Meazza C and Scanagatta P: Metastatic osteosarcoma: A challenging multidisciplinary treatment. Expert Rev Anticancer Ther 16: 543-556, 2016.
5. Kager L, Tamamyan G and Bielack S: Novel insights and therapeutic interventions for pediatric osteosarcoma. Future Oncol 13: 357-368, 2017.
6. Wang S, Zhong L, Li Y, Xiao D, Zhang R, Liao D, Lv D, Wang X, Wang J, Xie X, *et al*: Up-regulation of PCOLCE by TWIST1 promotes metastasis in Osteosarcoma. Theranostics 9: 4342-4353, 2019.
7. Kurosawa S: Anesthesia in patients with cancer disorders. Curr Opin Anaesthesiol 25: 376-384, 2012.
8. Guerrero Orriach JL, Raigon Ponferrada A, Malo Manso A, Herrera Imbroda B, Escalona Belmonte JJ, Ramirez Aliaga M, Ramirez Fernandez A, Diaz Crespo J, Soriano Perez AM, Fontaneda Heredia A, *et al*: Anesthesia in combination with propofol increases disease-free survival in bladder cancer patients who undergo radical tumor cystectomy as compared to inhalational anesthetics and opiate-based analgesia. Oncology 98: 161-167, 2020.
9. Jun IJ, Jo JY, Kim JI, Chin JH, Kim WJ, Kim HR, Lee EH and Choi IC: Impact of anesthetic agents on overall and recurrence-free survival in patients undergoing esophageal cancer surgery: A retrospective observational study. Sci Rep 7: 14020, 2017.
10. Sahinovic MM, Struys MMRF and Absalom AR: Clinical pharmacokinetics and pharmacodynamics of propofol. Clin Pharmacokinet 57: 1539-1558, 2018.
11. Xu Y, Pan S, Jiang W, Xue F and Zhu X: Effects of propofol on the development of cancer in humans. Cell Prolif 53: e12867, 2020.
12. Li R, Liu H, Dilger JP and Lin J: Effect of propofol on breast cancer cell, the immune system, and patient outcome. BMC Anesthesiol 18: 77, 2018.
13. Li H, Lu Y, Pang Y, Li M, Cheng X and Chen J: Propofol enhances the cisplatin-induced apoptosis on cervical cancer cells via EGFR/JAK2/STAT3 pathway. Biomed Pharmacother 86: 324-333, 2017.
14. Xu W, Zheng J, Bie S, Kang L, Mao Q, Liu W, Guo J, Lu J and Xia R: Propofol inhibits Wnt signaling and exerts anticancer activity in glioma cells. Oncol Lett 16: 402-408, 2018.
15. Huang YH, Wu ZF, Lee MS, Lou YS, Wu KL, Cheng KI and Lai HC: Propofol-based total intravenous anesthesia is associated with better survival than desflurane anesthesia in glioblastoma surgery. PLoS One 16: e0255627, 2021.
16. Cata JP and Forget P: Paravertebral block with propofol anaesthesia does not improve survival compared with sevoflurane anaesthesia for breast cancer surgery: Independent discussion of a randomised controlled trial. Br J Anaesth 124: 19-24, 2020.
17. Farooqi AA, Adylova A, Sabitaliyevich UY, Attar R, Sohail MI and Yilmaz S: Recent updates on true potential of an anesthetic agent as a regulator of cell signaling pathways and non-coding RNAs in different cancers: Focusing on the brighter side of propofol. Gene 737: 144452, 2020.
18. Peng X, Li C, Yu W, Liu S, Cong Y, Fan G and Qi S: Propofol attenuates hypoxia-induced inflammation in BV2 microglia by inhibiting oxidative stress and NF-κB/Hif-1α signaling. Biomed Res Int 2020: 8978704, 2020.
19. Yan HJ, Qi GQ and Ma Y: Effect of propofol on myocardial ischemia-reperfusion injury through MAPK/ERK pathway. Eur Rev Med Pharmacol Sci 23: 11051-11061, 2019.
20. Gao X, Mi Y, Guo N, Luan J, Xu H, Hu Z, Wang N, Zhang D, Gou X and Xu L: The mechanism of propofol in cancer development: An updated review. Asia Pac J Clin Oncol 16: e3-e11, 2020.
21. Xu YB, Jiang W, Zhao FR, Li G, Du QH, Zhang MY and Guo XG: Propofol suppresses invasion and induces apoptosis of osteosarcoma cell in vitro via downregulation of TGF-β1 expression. Eur Rev Med Pharmacol Sci 20: 1430-1435, 2016.

22. Huang X, Liu J and Xie H: Propofol suppresses osteosarcoma cell function by regulating FOXO1/TUSC7. J Pharm Pharmacol 73: 720-725, 2021.
23. Yun CW and Lee SH: The roles of autophagy in cancer. Int J Mol Sci 19: 3466, 2018.
24. Lin YC, Chen HY, Hsieh CP, Huang YF and Chang IL: Betulin inhibits mTOR and induces autophagy to promote apoptosis in human osteosarcoma cell lines. Environ Toxicol 35: 879-887, 2020.
25. Guo YN and Ma X: The effects of propofol on autophagy. DNA Cell Biol 39: 197-209, 2020.
26. Li F, Li F and Chen W: Propofol inhibits cell proliferation, migration, and invasion via mir-410-3p/transforming growth factor-β receptor type 2 (TGFBR2) Axis in glioma. Med Sci Monit 26: e919523, 2020.
27. Sun H and Gao D: Propofol suppresses growth, migration and invasion of A549 cells by down-regulation of miR-372. BMC Cancer 18: 1252, 2018.
28. Ye Z, Jingzhong L, Yangbo L, Lei C and Jiandong Y: Propofol inhibits proliferation and invasion of osteosarcoma cells by regulation of microRNA-143 expression. Oncol Res 21: 201-207, 2013.
29. Kansara M, Teng MW, Smyth MJ and Thomas DM: Translational biology of osteosarcoma. Nat Rev Cancer 14: 722-735, 2014.
30. Lilienthal I and Herold N: Targeting molecular mechanisms underlying treatment efficacy and resistance in osteosarcoma: A review of current and future strategies. Int J Mol Sci 21: 6885, 2020.
31. Zheng X, Wang Y, Dong L, Zhao S, Wang L, Chen H, Xu Y and Wang G: Effects of propofol-based total intravenous anesthesia on gastric cancer: A retrospective study. Onco Targets Ther 11: 1141-1148, 2018.
32. Wu ZF, Lee MS, Wong CS, Lu CH, Huang YS, Lin KT, Lou YS, Lin C, Chang YC and Lai HC: Propofol-based total intravenous anesthesia is associated with better survival than desflurane anesthesia in colon cancer surgery. Anesthesiology 129: 932-941, 2018.
33. Wu X, Liu JM, Song HH, Yang QK, Ying H, Tong WL, Zhou Y and Liu ZL: Aurora-B knockdown inhibits osteosarcoma metastasis by inducing autophagy via the mTOR/ULK1 pathway. Cancer Cell Int 20: 575, 2020.
34. Sun B, Ou H, Ren F, Huan Y, Zhong T, Gao M and Cai H: Propofol inhibited autophagy through Ca^{2+}/CaMKKβ/AMPK/mTOR pathway in OGD/R-induced neuron injury. Mol Med 24: 58, 2018.
35. Wang Y, Xu B, Zhou J and Wu X: Propofol activates AMPK to inhibit the growth of HepG2 cells in vitro and hepatocarcinogenesis in xenograft mouse tumor models by inducing autophagy. J Gastrointest Oncol 11: 1322-1332, 2020.
36. Zhang YF, Li CS, Zhou Y and Lu XH: Propofol facilitates cisplatin sensitivity via lncRNA MALAT1/miR-30e/ATG5 axis through suppressing autophagy in gastric cancer. Life Sci 244: 117280, 2020.
37. Zhao Y, Yang J, Liao W, Liu X, Zhang H, Wang S, Wang D, Feng J, Yu L and Zhu WG: Cytosolic FoxO1 is essential for the induction of autophagy and tumour suppressor activity. Nat Cell Biol 12: 665-675, 2010.
38. Zhao Y, Li X, Cai MY, Ma K, Yang J, Zhou J, Fu W, Wei FZ, Wang L, Xie D and Zhu WG: XBP-1u suppresses autophagy by promoting the degradation of FoxO1 in cancer cells. Cell Res 23: 491-507, 2013.
39. Bai Y, Chen Y, Chen X, Jiang J, Wang X, Wang L, Wang J, Zhang J and Gao L: Trichostatin A activates FOXO1 and induces autophagy in osteosarcoma. Arch Med Sci 15: 204-213, 2019.
40. Chen X, Li K and Zhao G: Propofol Inhibits HeLa cells by impairing autophagic flux via AMP-Activated protein kinase (AMPK) activation and endoplasmic reticulum stress regulated by calcium. Med Sci Monit 24: 2339-2349, 2018.